

Real-time Magnetometer Disturbance Estimation via Online Nonlinear Programming

Jin Wu, *Member, IEEE*

Abstract—Magnetometer is a significant sensor for integrated navigation. However, it suffers from many kinds of unknown dynamic magnetic disturbances. We study the problem of online estimating such disturbances via a nonlinear optimization aided by intermediate quaternion estimation from inertial fusion. The proposed optimization is constrained by geographical distribution of magnetic field forming a constrained nonlinear programming. The uniqueness of the solution has been verified mathematically and we design an interior-point-based solver for efficient computation on embedded chips. It is claimed that the designed scheme mainly outperforms in dealing with the challenging bias estimation problem under static motion as previous representatives can hardly achieve. Experimental results demonstrate the effectiveness of the proposed scheme on high accuracy, fast response and low computational load.

Index Terms—Magnetic Disturbance, Integrated Navigation, Quaternion, Nonlinear Programming, Interior-Point Method

I. INTRODUCTION

THREE-axis magnetometer is a crucial component in current mechatronic navigation and control applications [1], [2]. It is frequently employed for autonomous heading determination in robotics, which is an important preliminary for further estimation of velocity and position.

In orientation estimation, magnetometer can be easily interfered by outer electromagnetic disturbances generated by hard-iron objects, complicated operating environments and time-varying electric currents from motors and transmission wires [3], [4]. Extensive studies have been performed to solve the problem of offline magnetometer calibration and alignment to inertial sensors [5], [6]. However, offline calibration can not fix the issue of online unknown magnetic disturbance. Among many existing robust attitude estimation algorithms, to deal with unknown magnetic disturbances, there have been quite a lot using intelligent detection of anomalies along with covariance adaption of sensed magnetic field [7], [8]. Adaptive covariance estimation is practical in engineering applications but can not fully eliminate the effect of disturbance imposed on the steady-state results [9]. Such method can be treated as a dynamical weighting approach maximumly separating the distorted sensor measurements. Besides, magnetic outlier rejection, although proved to be feasible in high-end navigation systems comprising fiber-optic gyroscopes (FOGs), may also lead to long-term large heading drift for low-cost sensor arrays. Instead, more robust heading determination originates from estimating real-time magnetic disturbances. Online magnetic

disturbance estimation is not a new topic, but has been studied long ago for spacecraft missions [10]. Current results sometimes require the geomagnetic model information and needs long time (hour level) to converge to the simulated true values [11]. Recently, the concept of online calibration of magnetometer and alignment to inertial sensors has become a novel and leading tool, which can be achieved via Kalman filtering design [12] for full-parametric real-time calibration including scale factors, misalignments and biases. Simpler methods with less estimation parameters for low-cost sensors have been implemented recently using an extended Kalman filter (EKF) as well [13].

The joint limitation of [12] and [13] is that they cannot deal with static estimation of magnetic disturbances. Rather, representative motions have to be designed to obtain precise calibration results. In fact, for most cases, with magnetic disturbances within full measurement range, the magnetometer can hardly be magnetized and only the online sensor bias is required for heading compensation, which describes the good nonlinearity within sensor measurement saturation. As such, Fedele et al. proposed an asymptotic observer based on Volterra integral with the aid of angular rate measurements [14]. It also remains the shortcoming of mandatory distinctive angular motions and cannot instantly obtain the magnetic disturbance since a long window of historical magnetic sensing values is needed. Sophisticated generalized inverse imposed on the large window also highly increases the computational and storage burdens. Representative motions can only be conveniently applied to those cases when the sensors can be rotated and translated. However, for large-scale unmanned aerial vehicles (UAVs) and autonomous underwater vehicles (AUVs), it is very difficult for engineers to uninstall significant sensors or generate distinctive representative motions.

Based on limitations shown above, this paper proposes a novel online magnetic disturbance estimator using nonlinear programming. It mainly solves the problem of static estimation of unknown outer magnetic disturbances and also performs well in dynamic mode. It is mainly motivated by aligning the magnetically distorted attitude quaternion to a better reference one so that the disturbance may be estimated. The proposed solution utilizes an interior-point optimum searcher and has been implemented on embedded micro chips as well.

This paper is organized as follows: Section II contains the studied problem and our proposed optimization solution. Static and dynamic experiments are presented in Section III to show the superiority of the developed method. While concluding remarks are drawn in the last Section IV.

This research was supported by National Natural Science Foundation of China under grant 41604025. (Corresponding author: Jin Wu)

J. Wu is with Department of Electronic and Computer Engineering, Hong Kong University of Science and Technology, Hong Kong, China. e-mail: jin_wu_uestc@hotmail.

II. PROPOSED SOLUTION

A. Problem Formulation

The magnetometer measurement can be adequately modeled as follows [14]

$$\mathbf{M}^b = \hat{\mathbf{M}}^b + \mathbf{b}_{\text{dyn}} + \boldsymbol{\eta}_{\mathbf{M}^b} \quad (1)$$

in which \mathbf{M}^b is the measured magnetic field vector in the body frame b . The measurement is related with its true value $\hat{\mathbf{M}}^b$ by an additive unknown dynamic magnetic disturbance $\mathbf{b}_{\text{dyn}} = (b_{m_x}, b_{m_y}, b_{m_z})^T$ and a white-Gaussian noise $\boldsymbol{\eta}_{\mathbf{M}^b}$. The passive determination of \mathbf{b}_{dyn} can be reduced to estimating the true value $\hat{\mathbf{M}}^b$. In the following parts, we are going to do such estimation with the hypothesis that magnetometer measurements reflect the heading angle of the attached object while the heading information can also be acquired from other sensor fusion results e.g. inertial-only or vector-aided algorithms [15], [16]. First, we estimate the normalization of $\hat{\mathbf{M}}^b$. **We assume that** the employed magnetometer has been pre-calibrated for scale, misalignment and biases before onboard data sampling. This can actually be done by many offline means e.g. [17], [18], as also described in [14]. **Then it is assumed that** the the vehicle on which magnetometer is mounted moves within a section of local area without very large distance from origin (less than 500Km). In this way, $\|\hat{\mathbf{M}}^b\|$ can be regarded as constants fixed in the global Earth frame due to pre-calibration of magnetometer [14]. Then, the ideal magnetometer vector can be restored, from which the magnetic disturbance can be accordingly generated by $\mathbf{b}_{\text{dyn}} \approx \mathbf{M}^b - \hat{\mathbf{M}}^b$. When the vehicle runs with large distance, then the magnetometer norm $\|\hat{\mathbf{M}}^b\|$ can be also referenced from the International Geomagnetic Reference Field (IGRF, [19]) model provided that the global positioning information is known, such that [20]

$$\begin{aligned} \|\hat{\mathbf{M}}^b\|^2 = & \left[\sum_{n=1}^k \sum_{m=1}^n \left(\frac{a}{R_e} \right)^{n+2} \frac{\partial P_n^m(\cos \theta)}{\partial \theta} \times \right. \\ & \left. (g_n^m \cos m\varphi + h_n^m \sin m\varphi) \right]^2 + \\ & \left[\sum_{n=1}^k \sum_{m=1}^n \left(\frac{a}{R_e} \right)^{n+2} \frac{m P_n^m(\cos \theta)}{\sin \theta} \times \right. \\ & \left. (g_n^m \sin m\varphi - h_n^m \cos m\varphi) \right]^2 + \\ & \left[\sum_{n=1}^k \sum_{m=1}^n \left(\frac{a}{R_e} \right)^{n+2} (n+1) P_n^m(\cos \theta) \times \right. \\ & \left. (g_n^m \cos m\varphi + h_n^m \sin m\varphi) \right]^2 \end{aligned} \quad (2)$$

with a denoting the altitude with respect to the center of the Earth; R_e the standard equivalent Earth radius; θ and φ co-latitude and longitude angles in *rad*; P_n^m the associated Legendre function of degree m and order n ; k the approximation order; g_n^m and h_n^m Gaussian coefficients from global satellite geomagnetic measurements which are released in IGRF models announced per five or ten years.

B. The Proposed Nonlinear Programming

Assuming that at a certain time epoch we have measured the normalized vectors from accelerometer and magnetometer denoted as $\mathbf{a}^b = (a_x, a_y, a_z)^T$ and $\mathbf{m}^b = (m_x, m_y, m_z)^T = \hat{\mathbf{M}}^b / \|\hat{\mathbf{M}}^b\|$ respectively, the corresponding unnormalized attitude quaternion $\tilde{\mathbf{q}} = (\tilde{q}_0, \tilde{q}_1, \tilde{q}_2, \tilde{q}_3)^T$ can be computed as follows [21]

$$\begin{aligned} \tilde{q}_0 &= -a_y(m_N + m_x) + a_x m_y \\ \tilde{q}_1 &= (a_z - 1)(m_N + m_x) + a_x(m_D - m_z) \\ \tilde{q}_2 &= (a_z - 1)m_y + a_y(m_D - m_z) \\ \tilde{q}_3 &= a_z m_D - a_x m_N - m_z \end{aligned} \quad (3)$$

in which $m_D = a_x m_x + a_y m_y + a_z m_z$, $m_N = \sqrt{1 - m_D^2}$. Now applying

$$\begin{aligned} a_x^2 + a_y^2 + a_z^2 &= 1 \\ m_x^2 + m_y^2 + m_z^2 &= 1 \\ m_N^2 + m_D^2 &= 1 \end{aligned} \quad (4)$$

the quaternion norm can be given by

$$\|\tilde{\mathbf{q}}\| = 2\sqrt{m_N [(1 - a_z)(m_N + m_x) - a_x(m_D - m_z)]} \quad (5)$$

When the accelerometer and magnetometer are accurately aligned, the above quaternion determination owns very good precision for estimating m_N and m_D . As magnetic disturbances interfere the system, not only quaternion, but m_N and m_D will be distorted as well. The main motivation provided here is that when magnetic disturbances take place, the corresponding yaw and its rate will vary with heading information from quaternions and their derivatives given by inertial/aided fusion. The inertial/aided fusion can be used for checking rate consensus on yaw. Typically, with the zero-angular-rate update (ZARU, [22]) in static mode the quaternion from completely inertial fusion can maintain stable and accurate within short period, which is enough for magnetic disturbance compensation. In this way, by comparing the difference of two quaternions, the magnetic disturbances may be estimated.

Let us define the **magnetic vector restoration problem**: With given accelerometer vector \mathbf{a}^b , find \mathbf{m}^b to achieve the following minimization

$$\begin{aligned} \arg \min_{\mathbf{m}^b \in \mathbb{U}^3} & \left\{ \begin{aligned} & [-a_y(m_N + m_x) + a_x m_y - \|\tilde{\mathbf{q}}\| \hat{q}_0]^2 + \\ & [(a_z - 1)(m_N + m_x) + a_x(m_D - m_z) - \|\tilde{\mathbf{q}}\| \hat{q}_1]^2 + \\ & [(a_z - 1)m_y + a_y(m_D - m_z) - \|\tilde{\mathbf{q}}\| \hat{q}_2]^2 + \\ & [a_z m_D - a_x m_N - m_z - \|\tilde{\mathbf{q}}\| \hat{q}_3]^2 \end{aligned} \right\} \end{aligned} \quad (6)$$

provided that $\hat{\mathbf{q}} = (\hat{q}_0, \hat{q}_1, \hat{q}_2, \hat{q}_3)^T$ is the estimated quaternion from inertial/GNSS/visual/Lidar sensors [23], [24] exactly when the magnetometer is distorted and \mathbb{U}^3 denotes the set of all real 3-dimensional unitary vectors. **It is also noted that** the initial alignment of the yaw angle to true north has been performed before sensor fusion to eliminate the effect of magnetic declination. The local magnetic declination angle can also be referenced using local coordinates with IGRF model or even simply interpolate from empirical tables. Normally, the

declination angles can be referenced in advance with the rough knowledge of operating position by referencing declination tables from IGRF.

Such optimization aligns $\tilde{\mathbf{q}}$ to $\hat{\mathbf{q}}$ and obtains \mathbf{m}^b . It has two evident advantages [21]:

- 1) The roll and pitch are not affected by the magnetic measurements while accelerometer measurements will not influence the determination of heading.
- 2) The quaternion presented here is explicit and owns the simplest form and nonlinearities compared with all the other existing solutions.

To let $\tilde{\mathbf{q}}, \hat{\mathbf{q}}$ have the same roll and pitch information, the vector \mathbf{a}^b here is reconstructed using $\hat{\mathbf{q}}$. Then components of $\hat{\mathbf{q}}$ representing roll and pitch will only be intermediate variables without affecting the determination of \mathbf{m}^b . That is to say, the minimization (6) will compute the magnetic vector with all attention in the yaw direction. As the accelerometer/magnetometer is adequate for full attitude estimation, $\tilde{\mathbf{q}}$ can be aligned to any quaternion which depicts the feasibility of estimating \mathbf{m}^b from such minimization.

The current problem occurs that $\|\tilde{\mathbf{q}}\|$ may not always be real during optimization search. Besides, for the studied optimization (6), the estimated variables have to be bounded so that they would be reasonable physically and geographically. Furthermore, note that for a quaternion \mathbf{q} , both \mathbf{q} and its negative $-\mathbf{q}$ represent the same rotation [25]. While (3) can not always make sure that successive quaternions from accelerometer and magnetometer measurements are continuous. Based on above limitations, the optimization (6) is then revised by estimating magnetic vector \mathbf{m}^b along with the quaternion norm $k = \|\tilde{\mathbf{q}}\|$. The new programming is given by

$$\begin{aligned} \arg \min_{\begin{bmatrix} \mathbf{m}^b \\ k \end{bmatrix} \in \mathbb{R}^4} & \left\{ \begin{aligned} & [-a_y(m_N + m_x) + a_x m_y - k \hat{q}_0]^2 + \\ & [(a_z - 1)(m_N + m_x) + a_x(m_D - m_z) - k \hat{q}_1]^2 + \\ & [(a_z - 1)m_y + a_y(m_D - m_z) - k \hat{q}_2]^2 + \\ & [a_z m_D - a_x m_N - m_z - k \hat{q}_3]^2 \end{aligned} \right\} \\ \text{s.t.} & \begin{cases} \text{Inequalities: } \gamma_{m_D}^- < |m_D| < \gamma_{m_D}^+ \\ \gamma_k^- < |k| < \gamma_k^+ \\ \text{Equalities: (4) and } m_D = a_x m_x + a_y m_y + a_z m_z \end{cases} \end{aligned} \quad (7)$$

where $\gamma_{m_D}^+, \gamma_k^+$ and $\gamma_{m_D}^-, \gamma_k^-$ are upper and lower bounds for the variables m_D and k , respectively. The bounds $\gamma_{m_D}^+, \gamma_{m_D}^-$ are chosen according to the local magnetic dip angle [26] and k 's bounds are set based on the following criterion

$$\begin{aligned} \gamma_k^+ &= \beta_{\max} |a_z - 1| \\ \gamma_k^- &= \beta_{\min} |a_z - 1| \end{aligned} \quad (8)$$

where $\beta_{\max}, \beta_{\min} > 0$ are empirical constants for range scaling. Such criterion is according to the fact that $\lim_{a_z \rightarrow 1} \|\tilde{\mathbf{q}}\| = 0$ while in such condition

$$\lim_{a_z \rightarrow 1} \tilde{q}_0 = \lim_{a_z \rightarrow 1} \tilde{q}_1 = \lim_{a_z \rightarrow 1} \tilde{q}_2 = \lim_{a_z \rightarrow 1} \tilde{q}_3 = 0 \quad (9)$$

as well. For cases that $a_z \rightarrow 1$, the norm of quaternion will approach to very tiny values, then $\gamma_k^+, \gamma_k^- > 0$ are to ensure proper range for values of k guaranteeing non-existence of indefinite limits 0/0.

C. Uniqueness of Solution

Let us conduct the variable replacement by $\tilde{\mathbf{q}} - k\hat{\mathbf{q}} = \mathbf{P}\mathbf{x}$ where

$$\begin{aligned} \mathbf{x} &= (m_N + m_x, m_y, m_D - m_z, k)^T = (x_0, x_1, x_2, x_3)^T \\ \mathbf{P} &= \begin{bmatrix} -a_y & a_x & 0 & -\hat{q}_0 \\ a_z - 1 & 0 & a_x & -\hat{q}_1 \\ 0 & a_z - 1 & a_y & -\hat{q}_2 \\ -a_x & -a_y & a_z + 1 & -\hat{q}_3 \end{bmatrix} \end{aligned} \quad (10)$$

This indicates that the solution to the system $\tilde{\mathbf{q}} - k\hat{\mathbf{q}} = \mathbf{0}$ is equivalent to the null space of \mathbf{P} . However, it should be noted that here the null space of \mathbf{P} is not uniquely a column vector. Instead, it is composed by two perpendicular vectors. Here we would notice that the system of \mathbf{x}

$$\begin{cases} m_N + m_x = x_0 \\ m_y = x_1 \\ m_D - m_z = x_2 \end{cases} \quad (11)$$

fully depends on the independent programming governed by k . From another aspect, the system (11) can be transformed into quadratic form of m_x, m_y, m_z , which indicates there are two independent solutions as m_y is already determined. However, not all solutions can meet the requirements of the programming such that $\gamma_{m_D}^- < |m_D| < \gamma_{m_D}^+$. This reflects that the final optimal solution is still constrained by magnetic-field distribution of the geomagnetic model [26]. Then based on such constraint, the solved m_x, m_y, m_z will be unique in practice.

D. Interior-Point Method

As the solution to (7) can be uniquely determined, we introduce the interior-point method for solving the optimization. Let us define the optimization variable in (7) as $\mathbf{y} = [(\mathbf{M}^b)^T, k]^T$ and $f(\mathbf{y})$ denotes the scalar function to be minimized. Then all the constraints are tantamount to the standard form as follows

$$\begin{aligned} c_1(\mathbf{y}) &= (\gamma_{m_D}^+)^2 - m_D^2 > 0 \\ c_2(\mathbf{y}) &= m_D^2 - (\gamma_{m_D}^-)^2 > 0 \\ c_3(\mathbf{y}) &= (\gamma_k^+)^2 - k^2 > 0 \\ c_4(\mathbf{y}) &= k^2 - (\gamma_k^-)^2 > 0 \\ c_5(\mathbf{y}) &= m_x^2 + m_y^2 + m_z^2 = 1 \end{aligned} \quad (12)$$

By introducing the barrier parameter $\rho > 0$, the barrier function is defined by [27]

$$\mathcal{B}(\mathbf{y}, \rho) = f(\mathbf{y}) - \rho \{\ln[c_1(\mathbf{y})c_2(\mathbf{y})c_3(\mathbf{y})c_4(\mathbf{y})c_5(\mathbf{y})]\} \quad (13)$$

Now let us employ the Lagrangian multiplier $\boldsymbol{\lambda} = (\lambda_1, \lambda_2, \lambda_3, \lambda_4, \lambda_5)^T > 0$ which subjects to the Karush-Kuhn-Tucker (KKT) conditions defining the optimality of the nonlinear optimization, such that $c_i \lambda_i = \rho$ for $i = 1, 2, 3, 4, 5$. Then the gradient to the barrier function is computed by [27]

$$\begin{aligned} \mathbf{g} &= (g_0, g_1, g_2, g_3)^T = \\ \nabla f(\mathbf{y}) - \rho \sum_{i=1}^5 \frac{\nabla c_i(\mathbf{y})}{c_i(\mathbf{y})} &= \nabla f(\mathbf{y}) - \mathbf{G}^T \boldsymbol{\lambda} \end{aligned} \quad (14)$$

where $\mathbf{G} = \nabla[c_1(\mathbf{y}), c_2(\mathbf{y}), c_3(\mathbf{y}), c_4(\mathbf{y}), c_5(\mathbf{y})]^T$. Finally the interior-point method seeks proper searching direction $\boldsymbol{\pi} = (\boldsymbol{\pi}_y^T, \boldsymbol{\pi}_\lambda^T)$ by steepest gradient via the following system [27]

$$\begin{Bmatrix} \nabla^2 \mathcal{B} \\ D \begin{pmatrix} \lambda_1 \\ \vdots \\ \lambda_5 \end{pmatrix} \mathbf{G} \end{Bmatrix} D \begin{bmatrix} -\mathbf{G}^T \\ c_1(\mathbf{y}) \\ \vdots \\ c_5(\mathbf{y}) \end{bmatrix} \boldsymbol{\pi} = \begin{Bmatrix} -\nabla f(\mathbf{y}) + \mathbf{G}^T \boldsymbol{\lambda} \\ \rho - c_1(\mathbf{y})\lambda_1 \\ \vdots \\ \rho - c_5(\mathbf{y})\lambda_5 \end{Bmatrix} \quad (15)$$

where D denotes the diagonal matrix. Choosing a step length $h > 0$, the optimization variables are updated by

$$(\mathbf{y}^T, \boldsymbol{\lambda}^T)^T = (\mathbf{y}^T, \boldsymbol{\lambda}^T)^T + h\boldsymbol{\pi} \quad (16)$$

As all the Jacobians and Hessians related can be analytically pre-computed, the only computation burden falls into the solution to (15) which can be efficiently solved via the singular value decomposition (SVD). In the initialization stage of the interior-point search, the initial value of \mathbf{y} is chosen as $\mathbf{y} = (0, 0, 0, 1)^T$. When the optimization progresses over time, the current estimate of $\mathbf{y}, \boldsymbol{\lambda}$ is calculated based on the previous optimal search for the purpose of improving computational efficiency.

III. EXPERIMENTAL RESULTS

In this section, we conduct experiments in static and dynamic modes where 'static' one consists no angular and translational motion while dynamic one contains quite distinctive motion and dynamic noises. All the experiments take place in Wuhan, China with the position of latitude and longitude of $E - 113^\circ 41' \sim 115^\circ 05'$, $N - 29^\circ 58' \sim 31^\circ 22'$ respectively. At such position, the theoretical values of m_N and m_D are $m_N = 0.64 \sim 0.69$, $m_D = -0.77 \sim -0.73$. The standard norm of the magnetic vector after calibration is $\|\hat{\mathbf{M}}^b\| = 0.38593$ Gauss. For our proposed method, we set the following parameters:

- 1) Inequality constraints: $\gamma_{m_D}^+ = 0.95, \gamma_{m_D}^- = 0.05$, $\beta_{\max} = 10^4, \beta_{\min} = 10$.
- 2) Optimization parameters: initial Lagrangian multiplier: $\boldsymbol{\lambda} = (1/5, 1/5, 1/5, 1/5, 1/5)$; barrier parameter: $\rho = 10^{-4}$; searching step length: $h = 10^{-5}$; maximum iterations: 50; equality constraint tolerance: 10^{-15} ; function value $f(\mathbf{y})$ tolerance: 10^{-30} .

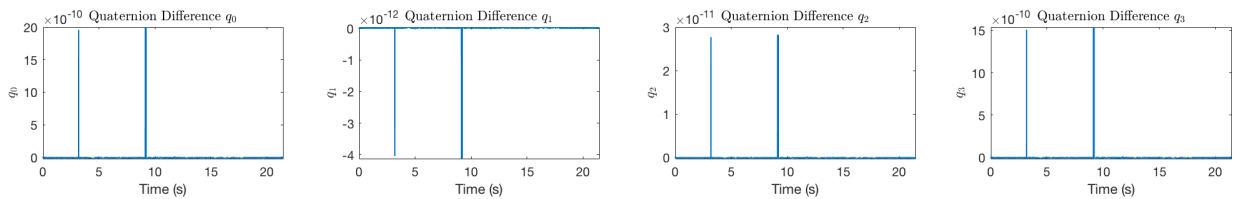


Fig. 5: Estimated quaternion differences.



Fig. 1: The measured magnetic field vectors from MTi-G-710 and 3DM-GX3-25 are distorted by an iron object.

The parameters are set very roughly to evaluate the robustness of the proposed algorithm. All the codes related to the proposed method are edited using the C++ programming language while the ALGLIB open-source optimization library of version 3.14.0 has been invoked for solving the proposed nonlinear programming. The codes are compiled via the GNU arm-eabi-g++-7.0 compiler for program execution on the embedded processing unit STM32H743VIT6. All the run-time performances in this paper are acquired from online computation on STM32H743VIT6 and stored via the SDIO high-speed bus. All the sensors referred to in this paper have underwent rigorous calibration for scale factors, misalignment, biases and etc.

A. Static Mode

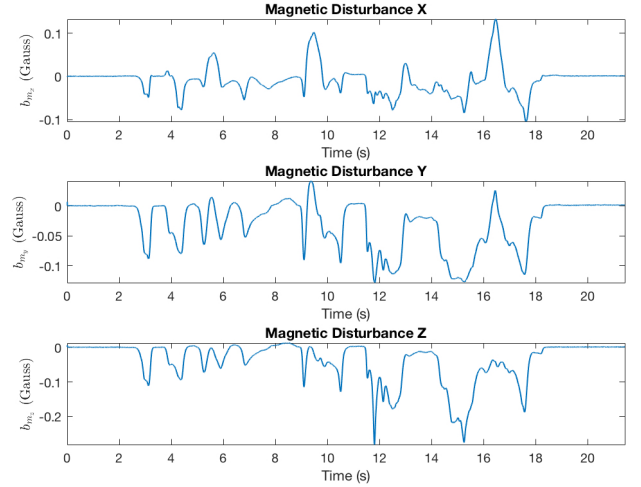


Fig. 2: Estimated magnetic disturbances.

In this sub-section, we face a challenging problem of estimating magnetic disturbances in static mode. In such case, the magnetometer stands still and no motion can be acquired to aid the estimation. There is no existing method that can instantly estimate in this situation. We use the hardwares presented in Fig. 1 to illustrate the performances. The Xsens MTi-G-710 integrated navigation product and 3DM-GX3-25 attitude and heading reference system all own internal high-precision 3-axis gyroscope, accelerometer and magnetometer. They are stucked firmly on a testing table and the sensor data of 3DM-GX3-25 has been aligned to that from MTi-G-710. According to Xsens's release notes, MTi-G-710's attitude estimation is prone to magnetic distortion in static mode while 3DM-GX3-25 does not have such functionality. Then based on these characteristics, the raw sensor readings are transmitted from 3DM-GX3-25 in 1000Hz and the readings of magnetometer are downsampled to 50Hz for adequate computational resources for nonlinear programming. The heading results from MTi-G-710 are employed as the source for true value of yaw angles. \hat{q} is obtained by the gyro-accelerometer fusion via a simple complementary filter [23]. We use a pair of pincers made of iron to make large magnetic distortion to the sensors. The testing table utilized here does not have any angular and translational motion which make the attached sensors in the fully static mode. With proposed method, the magnetic disturbances are estimated and shown in Fig. 2 while the raw magnetic vectors and compensated ones are depicted in Fig. 3. The quaternion alignment errors $\tilde{q}/k - \hat{q}$ are shown in Fig. 5.

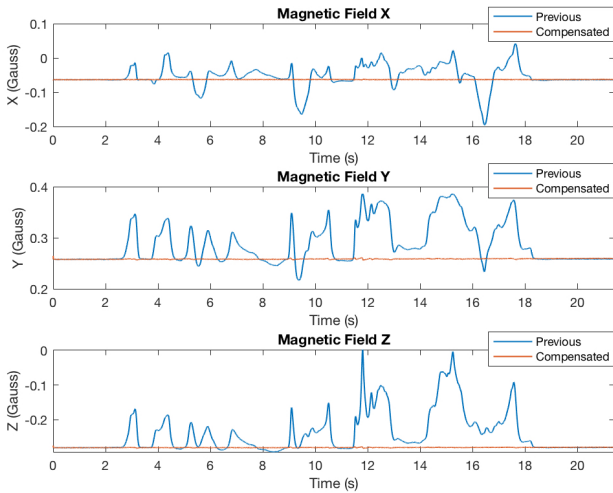


Fig. 3: Raw magnetic measurements and compensated ones.

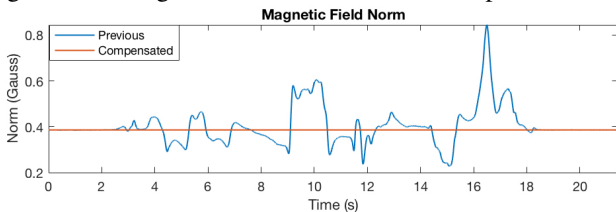


Fig. 4: Magnetic norms for previous and compensated magnetic vectors.

The magnetic disturbances generated here are completely

irregular. This can also be indicated by the norms of magnetometer measurements in Fig. 4. Moreover, the outer interferences vary instantly with motion of the iron object so previous asymptotically convergent observer can hardly immediately estimate the accurate disturbances. Our method, as a single-point optimizer, acts almost without any delay in such condition and outputs exactly accurate magnetic disturbances. From another side, traditional optimization methods for nonlinear programming are regarded as very slow in execution. However, even running on the embedded processor STM32H743VIT6 with clock speed of 400MHz, the proposed optimization can also accomplished the mission. Although the maximum iteration number has been set to 50, in all the logged runtime results, there is no iteration number over 27 (see Fig. 6). And under such times of iteration the core function values can be minimized to a large extent which produces very tiny values not over 5×10^{-29} . Such tiny values coincide with previous quaternion differences in Fig. 5. For one quaternion with error of 10^{-10} level, the magnitude of such errors can be totally ignored in practice. That is to say, the proposed method can estimate both computationally efficient and highly accurate magnetic disturbances.

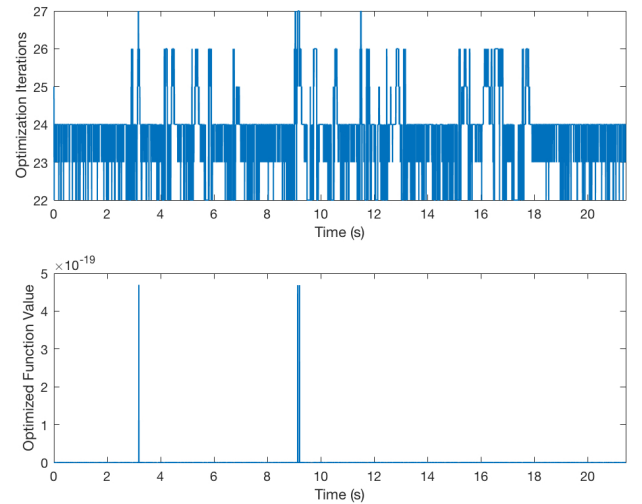


Fig. 6: Iteration numbers and minimized function values.

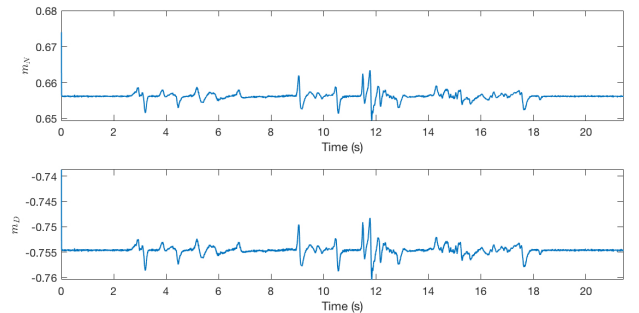


Fig. 7: Estimated m_N, m_D values.

Also, to verify the physical validity of the proposed method, we present the estimated m_N and m_D values in Fig. 7. As described in the beginning of this section, m_N, m_D are in their respective ranges characterized by the geomagnetic model.

The presented estimates in Fig. 7 well fall in such range which reflects its geographical correctness. It is also motivated that, since magnetic field can also be used for positioning in global Earth frame, then applying such estimates of m_N, m_D to previous estimators may also generate a rough information of the latitude, longitude and height. Such information may inversely help engineers to determine the quality of the estimation results.

B. Dynamic Mode

In this sub-section, dynamic experiments have been carried out on a self-designed remote operated vehicle (ROV, see Fig. 8) in underwater environment. The ROV employs the MTi-G-710 in last sub-section as the navigation sensor. The inertial data is sampled at 400Hz while for magnetometer the frequency is 50Hz. A moving iron-made 2DOF bed is hang over the pool to lead the bottom iron stick into the water (see Fig. 9). The ROV is operated via a ground control system with a joystick and we let it move freely in the water around the iron stick. The proposed scheme is enabled when detected angular rates from accelerometer and magnetometer are significantly less or larger than that from gyroscope (here threshold is set as $10^\circ/\text{hour}$).



Fig. 8: The designed ROV platform.

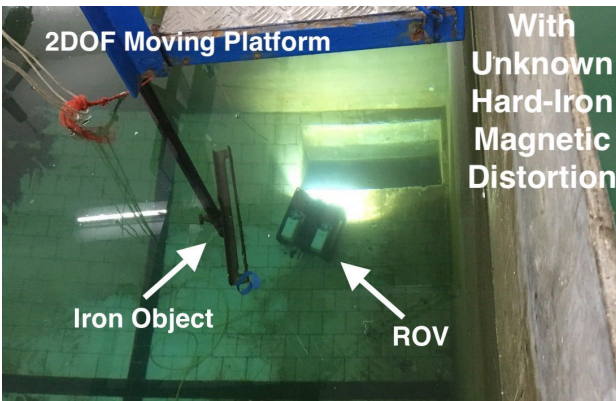


Fig. 9: Underwater experiment with iron-magnetic distortion.

In such scenario, the magnetometer is distorted both by the iron object and electric currents from thrusters. Such disturbances are generated by motors, which are regarded to be noisy. The proposed method accurately estimates the disturbances and then gives it back to raw sensor readings. Using the orientation method in [23], the heading angles before and after compensation are shown in Fig. 10. The proposed nonlinear programming can eliminate the magnetic disturbance in a fundamental manner. Therefore the heading determination can be significantly improved. The statistics of accuracy are shown in Table I.

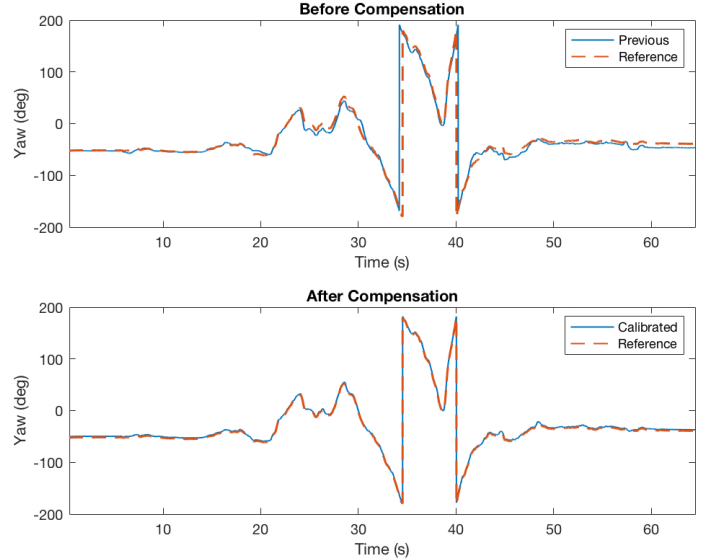


Fig. 10: Heading angles before and after compensation.

TABLE I: Root Mean Heading Accuracy

Before Compensation	After Compensation
12.89265227°	1.04376031°

As heading is extremely important for absolute navigation and control in global Earth frame, the proposed method may benefit to related applications in the future.

IV. CONCLUSION

In this paper, the magnetic disturbance estimation problem is studied. We propose a novel nonlinear optimization approach to solve such problem by means of the interior-point method. The uniqueness of the solution has been proven via mathematical constraints which ensures the effectiveness of the proposed method. Throughout real-world experiments, it has been validated to be correct, computationally efficient and it owns fast response facing unknown magnetic distortion. Future efforts should be devoted to obtaining more simplified optimization framework and faster calculation process to achieve better computational performance on low-cost and power-saving applications. It is also noted that the proposed method can only be effective for magnetometer data within full measurement range. Another task for us to accomplish

next is to study better algorithm under sensor saturation for more robust estimation performance.

ACKNOWLEDGMENT

This research was supported by National Natural Science Foundation of China under the grant of No. 41604025. We also genuinely thank Prof. Yuanxin Wu from Shanghai Jiao Tong University for his constructive comments.

REFERENCES

- [1] M. L. Psiaki, L. Huang, and S. M. Fox, "Ground tests of magnetometer-based autonomous navigation (MAGNAV) for low-earth-orbiting spacecraft," *Journal of Guidance, Control, and Dynamics*, vol. 16, no. 1, pp. 206–214, 1993.
- [2] A. M. Zanchettin, A. Calloni, and M. Lovera, "Robust magnetic attitude control of satellites," *IEEE/ASME Trans. Mech.*, vol. 18, no. 4, pp. 1259–1268, 2013.
- [3] L. Paull, S. Saeedi, M. Seto, and H. Li, "AUV navigation and localization: A review," *IEEE Journal of Oceanic Engineering*, vol. 39, no. 1, pp. 131–149, 2014.
- [4] M. S. Huq, R. Forrester, M. Ahmadi, and P. Straznicky, "Magnetic Characterization of Actuators for an Unmanned Aerial Vehicle," *IEEE/ASME Trans. Mech.*, vol. 20, no. 4, pp. 1986–1991, 2015.
- [5] Z.-Q. Zhang, "Two-Step Calibration Methods for Miniature Inertial and Magnetic Sensor Units," *IEEE Trans. Indu. Elec.*, vol. 62, no. 6, pp. 1–1, 2015.
- [6] Z.-q. Zhang and G.-z. Yang, "Micromagnetometer Calibration for Accurate Orientation Estimation," *IEEE Transactions on Biomedical Engineering*, vol. 62, no. 2, pp. 553–560, 2015.
- [7] J. Lee, J. Lim, and J. Lee, "Compensated Heading Angles for Outdoor Mobile Robots in Magnetically Disturbed Environments," *IEEE Trans. Indu. Elec.*, vol. 65, no. 2, pp. 1408–1419, 2017.
- [8] T. Beravs, S. Begus, J. Podobnik, and M. Munih, "Magnetometer Calibration Using Kalman Filter Covariance Matrix for Online Estimation of Magnetic Field Orientation," *IEEE Trans. Inst. Meas.*, vol. 63, no. 8, pp. 2013–2020, 2014.
- [9] B. Allotta, R. Costanzi, and F. Fanelli, "An Attitude Estimation Algorithm for Underwater Mobile Robots Under Unknown Magnetic Disturbances," *IEEE/ASME Trans. Mech.*, vol. 21, no. 4, pp. 1900–1911, 2016.
- [10] J. L. Crassidis, K.-L. Lai, and R. R. Harman, "Real-Time Attitude-Independent Three-Axis Magnetometer Calibration," *Journal of Guidance, Control, and Dynamics*, vol. 28, no. 1, pp. 115–120, 2005.
- [11] H. E. Söken and S.-i. Sakai, "Real-Time Attitude-Independent Magnetometer Bias Estimation for Spinning Spacecraft," *Journal of Guidance, Control, and Dynamics*, pp. 1–4, 2017.
- [12] Y. Wu, D. Zou, P. Liu, and W. Yu, "Dynamic Magnetometer Calibration and Alignment to Inertial Sensors by Kalman Filtering," *IEEE Trans. Contr. Syst. Tech.*, vol. 26, no. 2, pp. 716–723, 2018.
- [13] K. Han, H. Han, Z. Wang, and F. Xu, "Extended Kalman Filter-Based Gyroscope-Aided Magnetometer Calibration for Consumer Electronic Devices," *IEEE Sens. J.*, vol. 17, no. 1, pp. 63–71, 2017.
- [14] G. Fedele, L. D'Alfonso, and G. D'Aquila, "Magnetometer bias finite-time estimation using gyroscope data," *IEEE Trans. Aerosp. Elec. Syst.*, vol. 9251, no. c, 2018.
- [15] Y. Wu, J. Wang, and D. Hu, "A New Technique for INS / GNSS Attitude and Parameter Estimation Using Online Optimization," *IEEE Transactions on Signal Processing*, vol. 62, no. 10, pp. 2642–2655, 2014.
- [16] J. Wu, Z. Zhou, B. Gao, R. Li, Y. Cheng, and H. Fourati, "Fast Linear Quaternion Attitude Estimator Using Vector Observations," *IEEE Transactions on Automation Science and Engineering*, vol. 15, no. 1, pp. 307–319, 2018.
- [17] J. F. Vasconcelos, G. Elkaim, C. Silvestre, P. Oliveira, and B. Cardeira, "Geometric approach to strapdown magnetometer calibration in sensor frame," *IEEE Transactions on Aerospace and Electronic Systems*, vol. 47, no. 2, pp. 1293–1306, 2011.
- [18] D. Gebre-Egziabher, G. H. Elkaim, J. David Powell, and B. W. Parkinson, "Calibration of Strapdown Magnetometers in Magnetic Field Domain," *Journal of Aerospace Engineering*, vol. 19, no. April, pp. 87–102, 2006.
- [19] E. Thébault, C. C. Finlay, C. D. Beggan, P. Alken, J. Aubert, O. Barrois, F. Bertrand, T. Bondar, A. Boness, L. Brocco *et al.*, "International geomagnetic reference field: the 12th generation," *Earth, Planets and Space*, vol. 67, no. 1, p. 79, 2015.
- [20] M. Abdelrahman and S. Y. Park, "Simultaneous spacecraft attitude and orbit estimation using magnetic field vector measurements," *Aerospace Science and Technology*, vol. 15, no. 8, pp. 653–669, 2011.
- [21] J. Wu, Z. Zhou, H. Fourati, and Y. Cheng, "A Super Fast Attitude Determination Algorithm for Consumer-Level Accelerometer and Magnetometer," *IEEE Trans. Consum. Elec.*, vol. 64, no. 3, pp. 375–381, 2018.
- [22] A. R. J. Ruiz, F. S. Granja, J. C. P. Honorato, and J. I. G. Rosas, "Accurate pedestrian indoor navigation by tightly coupling foot-mounted imu and rfid measurements," *IEEE Transactions on Instrumentation and Measurement*, vol. 61, no. 1, pp. 178–189, 2012.
- [23] H. Fourati, N. Manamanni, L. Afilal, and Y. Handrich, "Complementary Observer for Body Segments Motion Capturing by Inertial and Magnetic Sensors," *IEEE/ASME Trans. Mech.*, vol. 19, no. 1, pp. 149–157, 2014.
- [24] F. Aghili and C.-Y. Su, "Robust Relative Navigation by Integration of ICP and Adaptive Kalman Filter Using Laser Scanner and IMU," *IEEE/ASME Trans. Mech.*, vol. 21, no. 4, pp. 1–1, 2016.
- [25] I. Y. Bar-Itzhack, "New Method for Extracting the Quaternion from a Rotation Matrix," *Journal of Guidance, Control, and Dynamics*, vol. 23, no. 6, pp. 1085–1087, 2000.
- [26] G. Shorshi and I. Y. Bar-Itzhack, "Satellite Autonomous Navigation Based on Magnetic Field Measurements," *Journal of Guidance, Control, and Dynamics*, vol. 18, no. 4, pp. 843–850, 1995.
- [27] J. Nocedal and S. J. Wright, "Numerical optimization second edition," 1999.